OsteoArthritis and Cartilage (2005) **13,** 971–978

doi:10.1016/j.joca.2005.06.015

Osteoarthritis and Cartilage

International Cartilage Repair Society

OARSI OSTEOARTHRITIS RESEARCH SOCIETY INTERNATIONAL

Cyclical articular joint loading leads to cartilage thinning and osteopontin production in a novel *in vivo* rabbit model of repetitive finger flexion[1]

K. B. King Ph.D.†‡*[2], C. F. Opel B.S.‡ and D. M. Rempel M.D., M.P.H.†‡

† *Department of Medicine, University of California, San Francisco, CA, USA*

‡ *Department of Bioengineering, University of California, Berkeley, CA, USA*

Summary

Objective: An *in vivo* rabbit model of repetitive joint flexion and loading was used to characterize the morphological effects of cyclical loading on articular cartilage.

Design: The forepaw digits of eight anesthetized New Zealand White adult female rabbits were repetitively flexed at 1 Hz with a mean peak digit load of 0.42 N for 2 h per day for 60 cumulative hours. Metacarpophalangeal joints were collected from loaded and contra-lateral control limbs, fixed, decalcified, embedded, and thin-sectioned. Serial sections were stained for histology or for immunohistochemistry. Morphometric data including the mean thicknesses of the uncalcified cartilage and of the calcified cartilage were collected from digital photomicrographs of safranin O-stained sections. The number of cells stained with anti-osteopontin antibody was counted.

Results: We observed a decrease in uncalcified cartilage mean thickness with no significant change in calcified cartilage thickness. We also observed a significant increase in the number of cells positive for osteopontin (OPN) in the uncalcified cartilage. These changes occurred without overt cartilage surface degeneration.

Conclusions: Cyclical loading leads to changes at the tissue and cellular levels in articular cartilage. These changes are suggestive of tidemark advancement and may indicate a reactivation of cartilage mineralization steps analogous to endochondral ossification. This novel *in vivo* rabbit model of repetitive flexion and loading can be used to investigate the effects of cyclical loading on articular joints.

Key words: Animal model, Mechanical loading, Cartilage biology, Remodeling, Osteopontin, *In vivo*.

Introduction

Multiple risk factors for osteoarthritis (OA) have been identified including familial OA, advanced age, obesity, prior injury, and occupation (reviewed by Felson[1]). The development and the progression of OA are mediated by multiple factors including genetics[2], epigenetics[3], biochemistry[4], and mechanics[5]. Understanding the specific role of each factor is important for treating OA and is vital for creating effective therapeutic interventions of the development and progression of OA. However, measuring the individual contribution of each of these factors in human subjects with OA is complicated by the often slow development of disease, the variability in symptom manifestation, and the difficulty of obtaining mild/early OA tissue biopsies with complete subject histories. In part to avoid these complications, *in vitro* and *in vivo* studies have been implemented to measure some of the specific factors that affect OA.

Mechanical factors such as compressive, tensile, and shear loading play important roles in articular joint health and disease. These have been studied using *in vitro* loading experiments (reviewed by DiMicco *et al.*[5]). Mechanical loading has also been studied using *in vivo* animal models. In some animal models joint loading is altered by surgically modifying the joint (e.g., ligament transection, full or partial menisectomy, osteotomy, or implantation of rods) often to create a slowly progressive degeneration similar to OA. In non-invasive models, the effects of cyclical loading are evaluated by joint immobilization or by training the animal to walk or run[6–10]; however, such methods cannot precisely control animal compliance or cycle frequency. These issues are overcome in the repetitive impulsive loading rabbit model (RIL model)[11,12]. However, the manner of loading simulates a sudden impact rather than the normal motions of joint flexion.

At this time, the beneficial and/or deleterious effects of non-traumatic compressive, tensile, and shear loading in combination are unclear. Such effects are relevant to the understanding, intervention, and prevention of degenerative joint diseases such as OA. For example, determining the relationship between compressive load levels and joint injury or between cumulative compression and injury may lead to recommendations for sports or workplace activities that can prevent injury.

[1] *Sources of support*: Centers for Disease Control and Prevention: National Institute of Occupational Safety and Health (Grant Number: OH007786); Northern California Chapter of the Arthritis Foundation; and Nathan & Violet David Scholars Program.

[2] University of California, San Francisco and at University of California, Berkeley.

*Address correspondence and reprint requests to: Karen B. King, Ph.D., University of California, Ergonomics Program, 1301 South 46th Street, Building 163, Richmond, CA 94804. Tel: 1-510-231-9448; Fax: 1-510-231-5729; E-mail: kbking@itsa.ucsf.edu

Received 8 December 2004; revision accepted 30 June 2005.

Our hypothesis is that physiologic, *in vivo* cyclical loading causes structural and metabolic changes in cartilage. To test this hypothesis, we created a novel *in vivo* rabbit model of precise repetitive joint flexion and loading and measured morphometric features of the articular cartilage and the presence of osteopontin (OPN) in both the loaded and non-loaded, contra-lateral control joints.

Method

STUDY DESIGN OVERVIEW

We developed a rabbit model in which the metacarpophalangeal (MCP) joint is repetitively flexed and loaded through electrical stimulation of the large finger flexor. The rabbit was selected because a rabbit's paw is similar to the human hand in general anatomy and tissue structures (e.g., bones of the digit, tendon attachments) when scaled for size. Rabbits have been used as *in vivo* models for human hand musculoskeletal disorders[13] and for testing hand surgery techniques[14]. Eight female, adult New Zealand White rabbits (3.5–4.0 kg) were loaded in individual sessions. Estimated age of the rabbits was approximately 6 months at the start of the study. The loading frequency was 1 Hz, the loading rate was 4.2 N/s, and the applied mean peak force at the digit was 0.42 N. Each rabbit received 2 h of digit flexion 3 days per week for a cumulative 60 h. The resultant load was selected to be within the physiologic range of the muscle and frequency of motion experienced by workers who perform repeated tasks[15]. These parameters were scaled to the rabbit size and muscle force. A previous study indicated that the 6 h per week of anesthesia was sustainable over a long duration without leading to hepatic, pulmonary, or circulatory complications[16]. In short-term pilot studies, cyclical loading of the flexor digitorum profundus (FDP) muscle was not consistently sustainable beyond 3 h at one time because muscle fatigue occurred. Rabbit weight, joint motion, and pain (reaction to palpitation of paw) were monitored and found normal throughout the experimental series. Outcome measures were made from stained tissue sections of the MCP joint within the cartilage covering palmar side of the distal end of the metacarpal bone within $\sim$500 μm of the joint border. All procedures were in compliance with the principles of "Guide for the Care and Use of Animals," and received prior approval and oversight from the University of California's Care and Use of Animals Committee.

IN VIVO RABBIT JOINT LOADING MODEL

The rabbit was anesthetized with isofluorane ($\sim$3% continuous, Henry Schein, Inc., Melville, NY) by mask (Anesthesia Service and Equipment, Inc., Jacksonville, FL) and placed supine on a heated pad with forelimbs supported at the mid-dorsal surface leaving the digits free. Vital signs were monitored continuously (ECG pulse oximeter, Heska Corp., Fort Collins, CO). A repetitive gripping motion was induced in one paw by electrical stimulation of the FDP muscle via a 33g stimulation needle placed subcutaneously in the mid-forelimb halfway between the wrist and elbow. A Grass-Telefactor stimulator (West Warwick, RI) was used to control muscle stimulation (1 train/s of 200 ms duration, 100 pulses/s of 1.0 ms duration). Only the FDP muscle was stimulated. A sham stimulation needle was inserted into the contra-lateral control limb but was not connected to the stimulator. Load was added to the tip of the third digit by sliding a lightweight brass cuff over the digit tip and connecting the cuff to a load cell with a stiff wire. The load cell output was displayed continuously at 1000 Hz on a computer monitor by a custom Labview program (National Instruments Corp., Austin, TX). The output was saved to computer disc periodically. The stimulation voltage was adjusted manually to maintain the target mean peak digit force. Following the experiments, the force histories from 3 randomly sampled days for each rabbit were averaged, and the actual mean peak force at the digit tip was determined to be 0.42 N.

The digit tip flexion force of 0.42 N was equivalent to 17.5% P_0, based on a pilot tetanic muscle force (P_0) experiment ($n = 4$ rabbits, between rabbit standard deviation (SD) $\pm$ 0.05 N). This test was analogous to the maximum voluntary contraction (MVC) commonly used to measure muscle strength in humans.

Biomechanical modeling of finger joint force by Chao *et al.*[17] predicted larger shear forces for the MCP compared to the other two joints and similar compressive forces for the MCP and proximal interphalangeal (PIP). Because the MCP joints were slightly larger than the PIP, the compressive stress was lower in the MCP than in the PIP. However, the larger size of the MCP provided more experimental tissue than the other joints. Therefore, the MCP joints were examined in this study.

HISTOLOGY

Rabbits were euthanized and the MCP joints of the third digit were harvested from both limbs after 60 cumulative hours of loading were completed. These specimens were fixed in formalin, decalcified in ethylenediaminetetraacetic acid 2 or 3 weeks, dehydrated, embedded in paraffin, sectioned in the sagittal plane (7 μm), and mounted on microscope slides with three sections per slide. Thin sections of every fifth slide were stained with safranin O/fast green/iron hematoxylin. Chemicals and supplies were purchased from Fisher Scientific International, Inc. (Hampton, NH), Electron Microscopy Sciences (Hatfield, PA), or Sigma-Aldrich, Co. (St. Louis, MO) unless otherwise indicated.

IMAGE ANALYSIS

Specimen handling, slide preparation, digital microphotography and image analysis were performed blinded to limb loading status.

To quantify morphological features, six of the stained slides from the central region of each MCP specimen were selected. Microscopic digital images of stained sections were captured for image analysis (Axioskop 2 MOT microscope and AxioCam digital camera, Carl Zeiss, Germany). A region of interest (ROI, 300 μm $\times$ 500 μm) was outlined on each image on the palmar side of the proximal (metacarpal) articular surface. The long axis of the ROI was placed parallel to the joint surface. This ROI was chosen based on a pilot study ($n = 4$ rabbits) in which cartilage thickness in this area decreased.

AxioVision software (Carl Zeiss) was used to measure articular cartilage area. The uncalcified cartilage area of the ROI was defined by the joint surface, the tidemark between the uncalcified and calcified cartilage, and the two edges of the ROI. The uncalcified cartilage mean thickness was calculated as the area divided by the width of the ROI (500 μm). The calcified cartilage area of the ROI was defined by the tidemark, the osteochondral junction, and the two edges of the ROI. The calcified cartilage mean

thickness was calculated as the respective area divided by the width of the ROI (500 μm).

IMMUNOHISTOLOGY

Thin sections were pretreated with hyaluronidase (Type IS, 600 U/ml in phosphate-buffered saline (PBS), pH 5.0, 10 min, 37°C) to improve antigen accessibility, followed by treatment with hydrogen peroxide to quench endogenous peroxidase activity (1% v/v in PBS, pH 7.2, 10 min, room temperature). Non-specific binding sites were blocked in diluted normal serum (30 min, room temperature) prior to overnight incubation with primary anti-OPN antibody (1 μg/ml at 4°C). Antigen–antibody binding was identified following manufacturer's protocols using horseradish peroxidase and Nova Red substrate (VectaStain ABC, Vector Lab, Burlingame, CA). The protocol for the negative control immunohistochemical experiment was identical but that the primary antibody was omitted. The sections from one rabbit were damaged and not analyzed.

The monoclonal anti-OPN antibody, "2A1," was a kind gift of Dr David Denhardt, Rutgers University. The antibody was prepared using purified recombinant OPN as described by D'Alonzo *et al.*[18]; when used on histological preparations the antibody recognizes a highly conserved epitope in the C-terminal half of the protein[19,20].

Digital microphotographs were captured as described above. The number of cells with antigenic staining and the number of cells without antigenic staining were counted. Cell density was calculated.

QUALITATIVE ANALYSIS

Other histological details related to joint pathology were noted for the cartilage of the entire joint. These included the presence of cartilage surface delamination or fibrillation, osteophyte formation, tidemark duplication, blood vessels in the cartilage, and safranin O staining density.

DATA ANALYSIS

The morphometric data were summarized as the means of six sections per joint for each outcome measure. These means appeared normally distributed. The means are reported ± SD of the mean. The OPN data were from one section per joint. For the determination of statistical significance, two-tailed, paired Student's *t* tests were used to compare loaded and contra-lateral control specimens ($n = 8$ rabbits for morphometric measures, $n = 7$ rabbits for OPN). The statistical significance level (α) was ≤ 0.05. Tests were performed using Sigma Plot v. 8.1 (Systat Software, Inc., Richmond, CA).

Results

GROSS HISTOLOGICAL FINDINGS

Typical histologic findings from the experimental and control joints of one rabbit are presented in Fig. 1. The articulating cartilage surfaces of all sections were intact without delamination or fibrillation including the regions not used for quantitative findings. The cartilage tissue of all sections stained evenly with safranin O, suggesting that a net loss of proteoglycans did not occur. Osteophytes were not observed. A duplicated tidemark was noted in at least one section of most specimens (seven of eight joints from both control and loaded limbs). A blood vessel either crossing or abutting the osteochondral junction was noted in at least one section of most specimens (seven of eight joints from control and loaded limbs). No blood vessels were observed in the uncalcified cartilage of either limb.

MEAN THICKNESS OF UNCALCIFIED AND CALCIFIED CARTILAGE

The uncalcified cartilage mean thickness and the calcified cartilage mean thickness were measured individually (Table I). The change in calcified cartilage mean thickness did not meet our statistical criteria ($\alpha \leq 0.05$). Total cartilage mean thickness (calculated as the sum of the uncalcified and the calcified mean thicknesses; $P = 0.08$) also did not meet our statistical criteria since these data were diluted by the calcified data. However, the decrease in the uncalcified cartilage mean thickness ($P = 0.03$) did meet our statistical criteria. In seven of eight rabbits the uncalcified cartilage mean thickness was less in the loaded limb compared to the contra-lateral control limb (Fig. 2).

OSTEOPONTIN

In the uncalcified cartilage, OPN staining was localized to the cell and its pericellular matrix (Fig. 3). In half of the joints some staining occurred at the joint surface, but this did not appear to be related to load status. No cells stained when the 2A1 antibody was omitted in the negative control immunohistology experiments.

The number of cells staining positive for OPN was greater in the loaded limb of seven rabbits compared to the control limb. The number of cells with antigenic staining and the number of those without were counted, and the density of OPN-stained cells was calculated. The mean number of positive cells per mm^2 of uncalcified cartilage was 0.89 (±0.7) in the control joint and 1.50 (±0.9) in the loaded joint ($P = 0.01$). The subject number was reduced because the control sections for rabbit 4 were damaged and not suitable for quantitative analysis.

We noted a difference in the baseline intensity of staining between rabbits. In the unloaded, control sections, overall staining was less intense for rabbits 1, 2, 3, and 4 than for rabbits 5, 6, 7, and 8. In the control sections, the mean density of positive cells for rabbits 1–3 was 0.25/mm^2 (±0.27), while for rabbits 5–8 the mean density positive was 1.37 cells/mm^2 (±0.41). The only difference in the treatment of specimens was that joints from rabbits 1–4 were decalcified for 2 weeks, while joints from rabbits 5–8 were decalcified for 3 weeks. The additional week of decalcification may have enhanced immunocytochemical staining with this antibody. However, since paired control and loaded joints from individual rabbits were decalcified and processed at the same duration, the difference in duration of decalcification did not affect the percent increase in the number of positive cells with loading. The increase with loading in the joints of rabbits 1–3 (68.4% ± 39.3) was similar to that of rabbits 5–8 (mean 70.1 ± 51.4). The percent increase in the density of OPN-positive cells for all seven rabbits was significant (mean 69.4% ± 42.9, $P = 0.01$).

Discussion

This is the first *in vivo* study to control the levels of both load and frequency of cyclical loading of articulating joints.

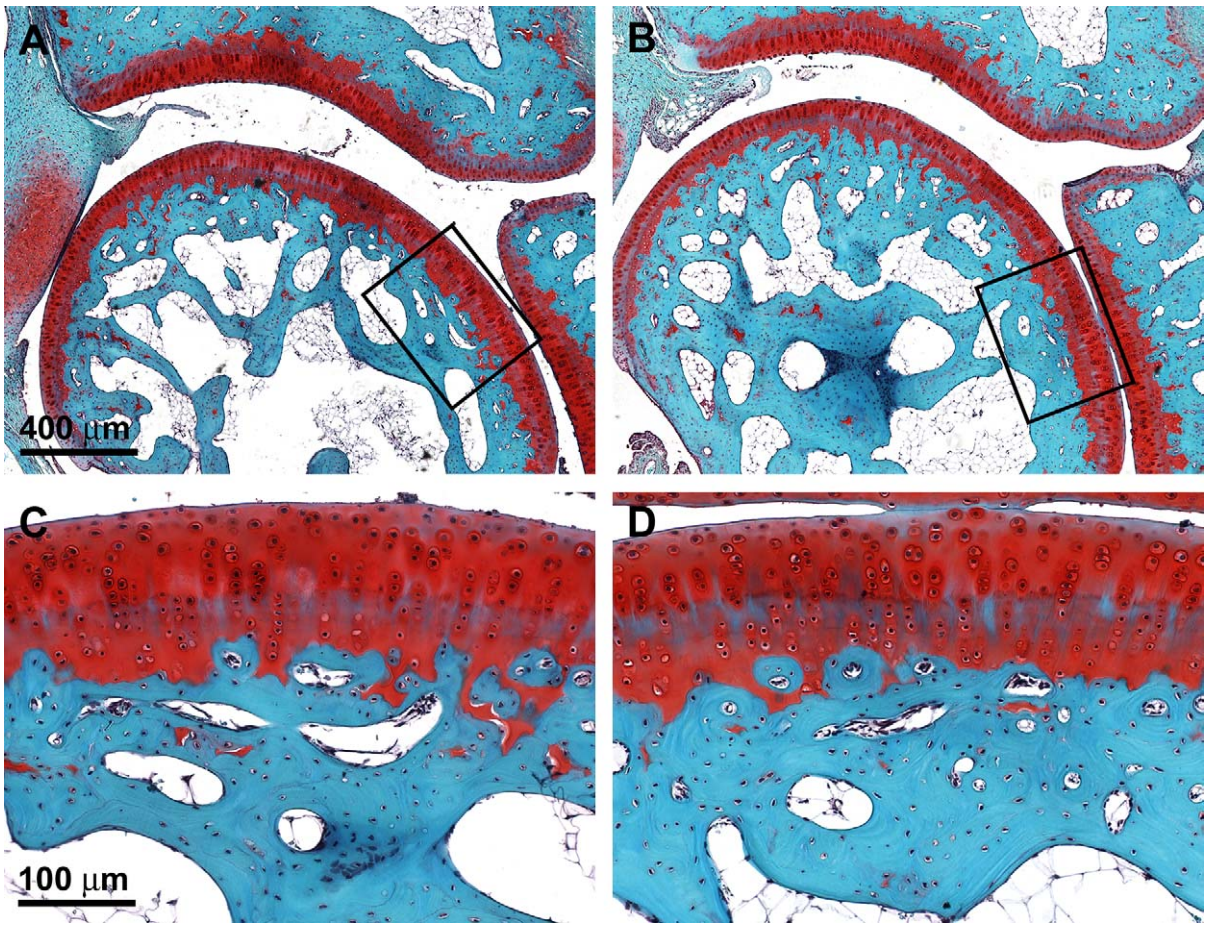

Fig. 1. Low (A,B) and high (C,D) magnification images of control (A,C) and loaded (B,D) MCP joint thin sections from the same rabbit stained with safranin O, fast green, and iron hematoxylin. In A and B the right side of the image is the palmar side of the joint and the bottom of the image is the proximal side of the joint. The boxed region in A and B indicate the locations of C and D, respectively.

Sixty cumulative hours of physiological loading leads to both structural (uncalcified cartilage thinning) and metabolic (increased OPN staining) changes to the cartilage.

There are three plausible mechanisms for the observed cartilage thinning. The first is tissue loss via degradation. However, we observe no cartilage surface delamination, no fibrillation, and no qualitative loss of proteoglycan staining (safranin O) in loaded joints. The histological methods used do not measure synthesis of proteoglycan which could maintain safranin O staining levels despite minor degradation. Increased synthesis of proteoglycan occurs with dynamic loading *in vitro*[5] and could be an effect of loading in the present study as well.

A second explanation is condensation of the tissue. This has been observed by others using *in vitro* cyclical compressive loading of osteochondral explants[21,22]. The change in cartilage volume may have been due to fluid loss from the unconfined explants. A quantitative *in vivo* magnetic resonance imaging (MRI) study demonstrates that dynamic knee bending decreases human patellar cartilage volume. This volume decrease reverses after 90 min of rest, which the authors attribute to temporary fluid loss and return[23]. Temporary fluid loss as a cause of tissue condensation in our model is unlikely since loading occurred over 10 weeks. Studies are in progress to determine if compaction of the collagen network is

Table I
Morphologic measures of articular cartilage after cyclical loading (n = 8 rabbits)

	Control limb ± SD	Experimental limb ± SD	Change* with load ± SD	Significance†
Uncalcified cartilage mean thickness (μm)	129.42 ± 26.8	115.64 ± 21.6	−9.70% ± 10.4	$P = 0.03$
Calcified cartilage mean thickness (μm)	78.15 ± 15.96	73.43 ± 7.64	−3.47% ± 16.9	$P = 0.37$
Total articular cartilage mean thickness (μm)	207.57 ± 40.2	189.06 ± 23.4	−7.55% ± 10.8	$P = 0.08$
Uncalcified cartilage portion of total mean thickness (%)	62.30 ± 3.8	60.89 ± 4.5	−2.18% ± 5.9	$P = 0.32$

*Percent change values are the means of the differences between experimental and control.
†Significance was determined using two-tailed paired *t* tests between control and experimental limbs.

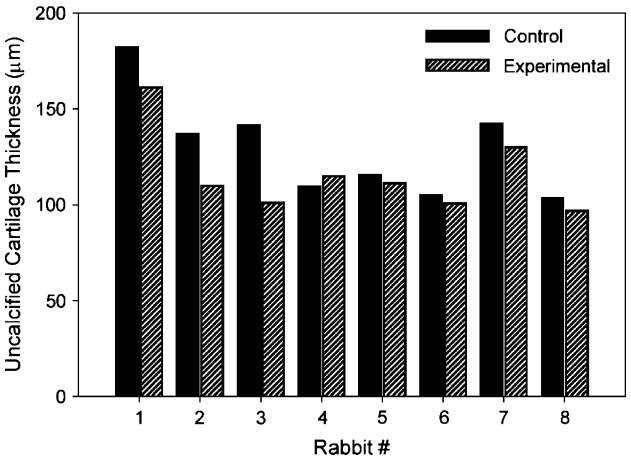

Fig. 2. Chart of mean thickness of uncalcified cartilage from each rabbit. Solid black bars indicate the control data (non-loaded limb). Bars with diagonal markings indicate the experimental data (loaded limb).

a contributing factor in uncalcified cartilage thinning in our model.

A third possible mechanism for uncalcified cartilage thinning is progressive mineralization of the uncalcified cartilage, sometimes called "tidemark advancement." The tidemark is a division in cartilage between the uncalcified and the calcified regions that continues to advance toward the joint surface, but very slowly, throughout life[24,25]. It has been demonstrated that mechanical load does affect mineralization. Lane and Bullough[26,27] demonstrate that tidemark advancement and subchondral plate remodeling via increased vascularity occur to a greater extent in regions of human humeral and femoral heads expected to be more highly loaded. We have not observed a net increase in vascularity with our methods. The shaved surface method used by Lane *et al.*[27] may be more sensitive to vascular measurement, but this method would inhibit our ability to perform immunohistology on serial sections.

If the tidemark moves from the calcified cartilage into the uncalcified, one might expect the mean thickness of the calcified cartilage to increase. For example, impact loading has been found to thicken calcified cartilage at the expense of the uncalcified cartilage[28]. In the present study, the

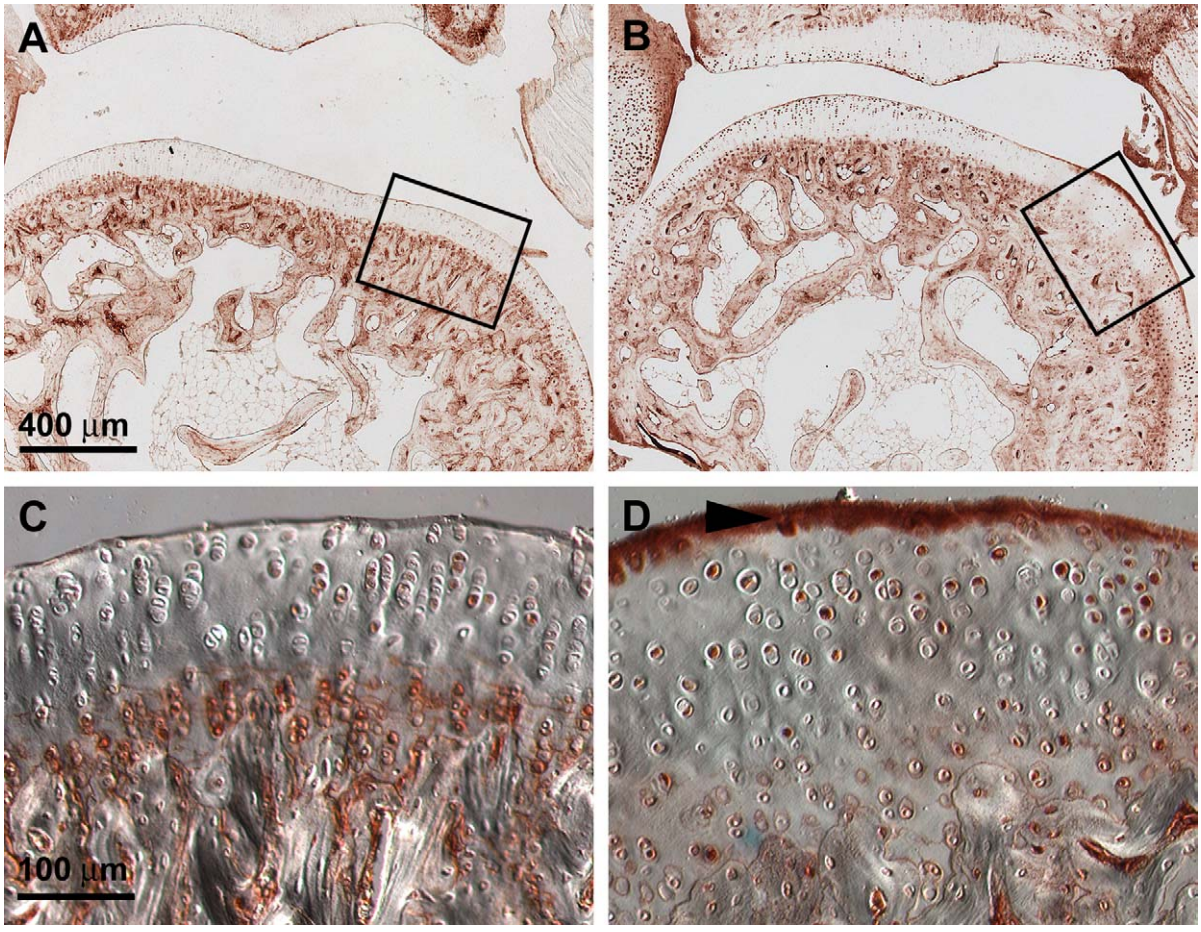

Fig. 3. Low (A,B) and high (C,D) magnification images of control (A,C) and loaded (B,D) MCP joint thin-sections from the same rabbit stained with anti-OPN antibodies. VectaStain ABC was used to visualize protein location (appears reddish brown). In A and B the right side of the image is the palmar side of the joint and the bottom of the image is the proximal side of the joint. The boxed region in A and B indicate the locations of C and D, respectively. Images C and D were captured using differential interference contrast filters (Carl Zeiss, Germany). The arrowhead in D marks staining of the superficial zone. Such staining appeared in an equal number of control and experimental sections and did not appear to be related to load status.

difference in mean calcified cartilage thickness is not statistically significant. However, the mean thickness of the calcified cartilage is dependant on the movement rate of both interfaces. Thus, if the rate of subchondral bone remodeling keeps approximate pace with the rate of tidemark advancement, then there is no net change in calcified cartilage mean thickness[26,28]. In addition, if both interfaces are moving toward the joint surface, the total cartilage mean thickness would decrease.

We propose that in the present study both interfaces are moving toward the joint surface. With 60 h of repetitive joint loading we observed a statistically significant decrease in uncalcified cartilage mean thickness ($P = 0.03$) and a trend for decrease in total cartilage mean thickness ($P = 0.08$). The calcified cartilage mean thickness may also be decreasing, but our observation was not statistically significant ($P = 0.37$). This lack of significance may be attributed to measurement error introduced by the undulation of the osteochondral interface. It should also be noted that the osteochondral interface itself may be remodeling with load.

With the present data, we are unable to state if one interface is moving at a faster rate than the other. If the tidemark were moving faster than the osteochondral interface, then the proportion of cartilage that is uncalcified would decrease significantly while that proportion which is calcified would increase. In the present study, such effects on proportions are not significant ($P = 0.32$). Therefore, the interface movement rates are either identical or similar enough to be indistinguishable with the present methods.

At present, tidemark advancement is one of three potential explanations that are not necessarily mutually exclusive. Further evidence to support a revival of endochondral ossification such as identification of mineralization markers is required.

Mineralization of the uncalcified cartilage would likely involve a change in phenotype of at least some of the uncalcified cartilage chondrocytes[29]. In our model, cyclical loading causes an increase in cellular OPN, a non-collagenous, sialic acid-rich phosphorylated matrix protein that contains the cell-binding amino acid sequence, Arg-Gly-Asp[30]. In the present study, the total number of OPN-positive cells as well as the number of positive cells per mm^2 increases with loading. We found a consistent increase in the percentage of cells with OPN staining in both groups, implying metabolic changes in the cells are occurring in response to mechanical loading. However, because the exact number of OPN-positive cells in the unloaded control joint can only be estimated, more investigation into the effect of decalcification should be performed. This response to mechanical loading has been demonstrated *in vivo* in bone[31,32]. Studies using bone cells in culture show increased OPN expression and synthesis due to loading, specifically to hydrostatic compressive loading[33] and to fluid flow[34,35]. Mitogen-activated protein kinases (MAPK) likely transduce the fluid flow stimulus for OPN gene expression in bone cells[35]. Our study is the first to examine the effect of mechanical load on OPN in adult articular chondrocytes. Here, too, fluid flow is relevant. Intermittent joint loading and motion causes fluid flow particularly in the upper cartilage zones[36]. We speculate that a signaling mechanism similar to that of bone may be involved. However, the exact role of OPN in cartilage is unknown.

The expression of OPN is thought to be inhibited in non-hypertrophic chondrocytes due to a negative promoter element as demonstrated in transgenic mice[37]. However, chondrocyte expression of OPN messenger RNA (mRNA) does occur in distraction osteogenesis in which tensile strain (0.5 mm/day) is applied to the healing cartilaginous callus resulting in endochondral ossification and subsequent bone formation[38]. Furthermore, OPN is produced by the chondrocytes of human OA cartilage with a correlation between OPN mRNA and the presence of cellular and territorial matrix OPN protein[39]. To answer whether the repetitive flexion and load-induced tidemark advance and OPN production are simply physiological adaptations or ultimately lead to pathological changes will require experiments of longer duration.

A disadvantage of our animal model is that under general anesthesia the skeletal muscles are flaccid[40], so there is no co-contraction and there is no muscle activity during digit extension (gravity and passive joint forces return the digits to resting posture). Due to the anesthesia, the loads are very similar, but not identical, to conscious repetitive motor activities. However, this model does allow precise control of mean peak load and repetition frequency, as well as control of other parameters such as rate of load, duty cycle, and total duration. This new *in vivo* model will not only aid our fundamental understanding of the mechanobiology of articular joint loading, but has the potential to advance our understanding of adult ossification by testing related hypotheses. For example, Carter *et al.*[36,41,42] postulate that shear stress promotes, but hydrostatic stress inhibits, mineralization. It may be that in our *in vivo* cyclical loading model a disruption of the normal ratio between intermittent shear stresses and intermittent hydrostatic stresses is responsible for accelerated tidemark advancement and subsequent thinning of the uncalcified cartilage.

Future studies using this model will benefit the interpretation of environmental impact on human OA studies, particularly the impact of subjects' occupational and athletic activities. This model also has the potential for exploring more damaging parameters such as higher force, greater frequency, and longer duration of joint loading. This may allow us to determine thresholds for injury (i.e., good loading vs bad loading) as suggested by *in vitro* studies[5]. Finally, because any successfully engineered tissue for joint repair must be functional for many years, knowledge of the *in vivo* effects of loading is critical. Future studies using this model will potentially benefit the design of joint tissue constructs and the design of post-implant therapy.

Acknowledgments

The authors thank Yuka Nakamura, Alex Portnoy, Alan Barr, and Michelle Lee for technical assistance.

References

1. Felson DT. Risk factors for osteoarthritis: understanding joint vulnerability. Clin Orthop Relat Res 2004:S16–21.
2. Loughlin J. Genetics of osteoarthritis and potential for drug development. Curr Opin Pharmacol 2003;3: 295–9.
3. Roach H, Inglis S, Clarke N, Oreffo R, Bronner F. Is osteoarthritis predominantly an epigenetic disease? Trans Orthop Res Soc 2005;30: paper 0248.
4. Heinegård D, Bayliss MT, Lorenzo P. Biochemistry and metabolism of normal and osteoarthritic cartilage. In: Brandt KD, Doherty M, Lohmander LS, Eds.

Osteoarthritis. New York: Oxford University Press 2003;73–82.
5. DiMicco MA, Kim Y-J, Grodzinsky AJ. Response of the chondrocyte to mechanical stimuli. In: Brandt KD, Doherty M, Lohmander LS, Eds. Osteoarthritis. New York: Oxford University Press, Inc. 2003; 112–20.
6. Norrdin RW, Kawcak CE, Capwell BA, McIlwraith CW. Subchondral bone failure in an equine model of overload arthrosis. Bone 1998;22:133–9.
7. Jortikka MO, Inkinen RI, Tammi MI, Parkkinen JJ, Haapala J, Kiviranta I, *et al*. Immobilisation causes longlasting matrix changes both in the immobilised and contralateral joint cartilage. Ann Rheum Dis 1997; 56:255–61.
8. Arokoski JPA, Hyttinen MM, Lapvetelainen T, Takacs P, Kosztaczky B, Modis L, *et al*. Decreased birefringence of the superficial zone collagen network in the canine knee (stifle) articular cartilage after long distance running training, detected by quantitative polarised light microscopy. Ann Rheum Dis 1996;55: 253–64.
9. Kiviranta I, Tammi M, Jurvelin J, Arokoski J, Saamanen A-M, Helminen HJ. Articular cartilage thickness and glycosaminoglycan distribution in the canine knee joint after strenuous running exercise. Clin Orthop 1992; 283:302–8.
10. Murray RC, Zhu CF, Goodship AE, Lakhani KH, Agrawal CM, Athanasiou KA. Exercise affects the mechanical properties and histological appearance of equine articular cartilage. J Orthop Res 1999;17: 725–31.
11. Radin EL, Parker HG, Pugh JW, Steinberg RS, Paul IL, Rose RM. Response of joints to impact loading. 3. Relationship between trabecular microfractures and cartilage degeneration. J Biomech 1973;6:51–7.
12. Radin EL, Ehrlich MG, Chernack R, Abernethy P, Paul IL, Rose RM. Effect of repetitive impulsive loading on the knee joints of rabbits. Clin Orthop 1978;131: 288–93.
13. Diao E, Shao F, Liebenberg E, Rempel D, Lotz JC. Carpal tunnel pressure alters median nerve function in a dose-dependent manner: a rabbit model for carpal tunnel syndrome. J Orthop Res 2005;23:218–23.
14. Jones ME, Burnett S, Southgate A, Sibbons P, Grobbelaar AO, Green CJ. The role of human-derived fibrin sealant in the reduction of postoperative flexor tendon adhesion formation in rabbits. J Hand Surg [Br] 2002;27:278–82.
15. Silverstein BA, Fine LJ, Armstrong TJ. Hand wrist cumulative trauma disorders in industry. Br J Ind Med 1986;43:779–84.
16. Nakama L, King K, Abrahamsson S, Rempel D. Evidence of tendon microtears due to cyclical loading in an *in vivo* tendinopathy model. J Orthop Res (In press).
17. Chao E, An K-N, Cooney W, Linscheid R. Biomechanics of the Hand: a Basic Research Study. Teaneck, NJ: World Scientific Publishing Co., Inc. 1989.
18. D'Alonzo RC, Kowalski AJ, Denhardt DT, Nickols GA, Partridge NC. Regulation of collagenase-3 and osteocalcin gene expression by collagen and osteopontin in differentiating MC3T3-E1 cells. J Biol Chem 2002;277: 24788–98.
19. Rittling SR, Chen Y, Feng F, Wu Y. Tumor-derived osteopontin is soluble, not matrix associated. J Biol Chem 2002;277:9175–82.
20. Kowalski AJ. Creation, characterization, and application of novel anti-osteopontin monoclonal antibodies. PhD thesis: "Cell Biology and Neuroscience." Piscataway, NJ: Rutgers University, 2005.
21. Kiraly K, Hyttinen MM, Parkkinen JJ, Arokoski JA, Lapvetelainen T, Torronen K, *et al*. Articular cartilage collagen birefringence is altered concurrent with changes in proteoglycan synthesis during dynamic *in vitro* loading. Anat Rec 1998;251:28–36.
22. Wong M, Siegrist M, Cao X. Cyclic compression of articular cartilage explants is associated with progressive consolidation and altered expression pattern of extracellular matrix proteins. Matrix Biol 1999;18:391–9.
23. Eckstein F, Tieschky M, Faber S, Englmeier KH, Reiser M. Functional analysis of articular cartilage deformation, recovery, and fluid flow following dynamic exercise *in vivo*. Anat Embryol (Berl) 1999;200:419–24.
24. Oegema TR Jr, Carpenter RJ, Hofmeister F, Thompson RC Jr. The interaction of the zone of calcified cartilage and subchondral bone in osteoarthritis. Microsc Res Tech 1997;37:324–32.
25. Patel N, Buckland-Wright C. Advancement in the zone of calcified cartilage in osteoarthritic hands of patients detected by high definition macroradiography. Osteoarthritis Cartilage 1999;7:520–5.
26. Lane LB, Bullough PG. Age-related changes in the thickness of the calcified zone and the number of tidemarks in adult human articular cartilage. J Bone Joint Surg Br 1980;62:372–5.
27. Lane LB, Villacin A, Bullough PG. The vascularity and remodelling of subchondral bone and calcified cartilage in adult human femoral and humeral heads. An age- and stress-related phenomenon. J Bone Joint Surg Br 1977;59:272–8.
28. Burr DB. Anatomy and physiology of the mineralized tissues: role in the pathogenesis of osteoarthrosis. Osteoarthritis Cartilage 2004;12(Suppl A):S20–30.
29. Gerstenfeld LC, Shapiro FD. Expression of bone-specific genes by hypertrophic chondrocytes: implication of the complex functions of the hypertrophic chondrocyte during endochondral bone development. J Cell Biochem 1996;62:1–9.
30. Oldberg A, Franzen A, Heinegard D. Cloning and sequence analysis of rat bone sialoprotein (osteopontin) cDNA reveals an ARG-GLY-ASP cell-binding sequence. Proc Natl Acad Sci U S A 1986;83: 8819–23.
31. Terai K, Takano-Yamamoto T, Ohba Y, Hiura K, Sugimoto M, Sato M, *et al*. Role of osteopontin in bone remodeling caused by mechanical stress. J Bone Miner Res 1999;14:839–49.
32. Morinobu M, Ishijima M, Rittling SR, Tsuji K, Yamamoto H, Nifuji A, *et al*. Osteopontin expression in osteoblasts and osteocytes during bone formation under mechanical stress in the calvarial suture *in vivo*. J Bone Miner Res 2003;18:1706–15.
33. Klein-Nulend J, Roelofsen J, Semeins CM, Bronckers AL, Burger EH. Mechanical stimulation of osteopontin mRNA expression and synthesis in bone cell cultures. J Cell Physiol 1997;170:174–81.
34. Owan I, Burr DB, Turner CH, Qiu J, Tu Y, Onyia JE, *et al*. Mechanotransduction in bone: osteoblasts are more responsive to fluid forces than mechanical strain. Am J Physiol 1997;273:C810–5.
35. You J, Reilly GC, Zhen X, Yellowley CE, Chen Q, Donahue HJ, *et al*. Osteopontin gene regulation by oscillatory fluid flow via intracellular calcium mobilization and activation of

mitogen-activated protein kinase in MC3T3-E1 osteoblasts. J Biol Chem 2001;276:13365–71.
36. Carter D, Beaupre G. Skeletal Function and Form: Mechanobiology of Skeletal Development, Aging, and Regeneration. New York: Cambridge University Press 2001.
37. Higashibata Y, Sakuma T, Kawahata H, Fujihara S, Moriyama K, Okada A, *et al*. Identification of promoter regions involved in cell- and developmental stage-specific osteopontin expression in bone, kidney, placenta, and mammary gland: an analysis of transgenic mice. J Bone Miner Res 2004;19:78–88.
38. Sato M, Yasui N, Nakase T, Kawahata H, Sugimoto M, Hirota S, *et al*. Expression of bone matrix proteins mRNA during distraction osteogenesis. J Bone Miner Res 1998;13:1221–31.
39. Pullig O, Weseloh G, Gauer S, Swoboda B. Osteopontin is expressed by adult human osteoarthritic chondrocytes: protein and mRNA analysis of normal and osteoarthritic cartilage. Matrix Biol 2000;19: 245–55.
40. Lipman N, Marini R, Flecknell P. Anesthesia and analgesia in rabbits. In: Kohn DF, Wixson SK, White WJ, Benson GJ, Eds. Anesthesia and Analgesia in Laboratory Animals. San Diego: Academic Press 1997;205–32.
41. Wong M, Carter DR. Articular cartilage functional histomorphology and mechanobiology: a research perspective. Bone 2003;33:1–13.
42. Carter DR, Wong M. The role of mechanical loading histories in the development of diarthrodial joints. J Orthop Res 1988;6:804–16.